Published in final edited form as:
Insect Biochem Mol Biol. 2008 May ; 38(5): 604–610. doi:10.1016/j.ibmb.2008.01.003.

Molecular and functional characterization of voltage-gated sodium channel variants from *Drosophila melanogaster*

Rachel O'Donnell Olson, **Zhiqi Liu**[1], **Yoshiko Nomura**, **Weizhong Song**, and **Ke Dong**[*]
Department of Entomology, Neuroscience Program and Genetics Program, Michigan State University, East Lansing, MI 48824, USA

Abstract

Extensive alternative splicing and RNA editing have been documented for the transcript of $DmNa_V$ (formerly *para*), the sole sodium channel gene in *Drosophila melanogaster*. However, the functional consequences of these post-transcriptional modifications are not well understood. In this study we isolated 64 full-length $DmNa_V$ cDNA clones from *D. melanogaster* adults. Based on the usage of 11 alternative exons, 64 clones could be grouped into 29 splice types. When expressed in *Xenopus* oocytes, 33 $DmNa_V$ variants generated sodium currents large enough for functional characterization. Among these variants, $DmNa_V$5-1 and $DmNa_V$7-1 channels activated at the most hyperpolarizing potentials, whereas $DmNa_V$1-6 and $DmNa_V$19 channels activated at the most depolarizing membrane potentials. We identified an A-to-I editing event in $DmNa_V$5-1 that is responsible for its uniquely low-voltage-dependent activation. The wide range of voltage dependence of gating properties exhibited by $DmNa_V$ variants represents a rich resource for future studies to determine the role of $DmNa_V$ in regulating sodium channel gating, pharmacology, and neuronal excitability in insects.

Keywords

Sodium channel; Alternative splicing; RNA editing; *Drosophila melanogaster*; Para; *Xenopus* oocyte expression system

1. Introduction

Voltage-gated sodium channels are integral transmembrane proteins responsible for the generation of action potentials across the membranes of excitable cells. Mammalian sodium channels consist of a large pore-forming α-subunit and one or more smaller auxiliary β-subunits. The α-subunit is composed of four homologous domains (I–IV), each containing six hydrophobic transmembrane segments (S1–S6). Mammals have nine α-subunit genes which encode sodium channel isoforms with different gating properties and different expression patterns in various cell types, tissues, and developmental stages, presumably to fulfill unique functions in specific neurons (Catterall, 2000; Goldin et al., 2000; Yu and Catterall, 2003). In contrast, insects appear to have only a single sodium channel gene, such as $DmNa_V$ (formerly *para*) in *Drosophila melanogaster*, encoding the equivalent of the α-subunit of the mammalian sodium channels (Loughney et al., 1989). The sodium channel β-subunits in insects are less well understood, except that a unique transmembrane protein, TipE, is required for robust expression of insect sodium channels in heterologous *Xenopus* oocytes (Feng etal., 1995; Warmke et al., 1997).

[*]Corresponding author. Tel.: + 1 517 432 2034; fax: +1 517 353 5598. dongk@msu.edu (K. Dong).
[1]Current address: ChanTest Inc., 14656 Neo Parkway, Cleveland, OH 44128, USA

Functionally distinct sodium currents have been documented in various insect neurons, indicating existence of heterogeneous sodium channels with distinct gating properties *in vivo* (Byerly and Leung, 1988; Lapied et al., 1990, 1999; Saito and Wu, 1991, [1993]; Schafer et al., 1994; O'Dowd, 1995; Le Corronc et al., 1999; Grolleau and Lapied, 2000; Wicher et al., 2001; Defaix and Lapied, 2005). A fundamental question is how insects produce heterogeneous sodium channels from a single gene. One possibility is that post-transcriptional modifications of the primary sodium channel transcript result in variations of sodium channel gating properties. Indeed, alternative splicing and RNA editing of the *DmNa*$_V$ transcript have been reported (O'Dowd and Aldrich, 1988; Loughney et al., 1989; Thackeray and Ganetzky, 1994, 1995; O'Dowd, 1995; Warmke et al., 1997; Palladino et al., 2000). The functional consequences of alternative splicing and/or RNA editing of the *DmNa*$_V$ transcript, however, remain largely unknown. Prior to this study, only one full-length *DmNa*$_V$ cDNA clone has been functionally characterized in *Xenopus* oocytes (Warmke et al., 1997).

Recent characterization of the German cockroach *BgNa*$_V$ sodium channel gene suggests that alternative splicing and RNA editing are two major mechanisms by which cockroaches produce functionally diverse sodium channels (Tan et al., 2002; Liu et al., 2004; Song et al., 2004; Dong, 2007). To determine whether alternative splicing- and RNA editing-mediated generation of diverse sodium channel gating properties is a common phenomenon in insects, we conducted a large-scale functional characterization of alternative splicing and RNA editing variants of the *D. melanogaster DmNa*$_V$ gene. Here, we report the isolation of 64 full-length *DmNa*$_V$ cDNA clones from *D. melanogaster* and functional characterization of these variants in *Xenopus* oocytes.

2. Materials and methods

2.1. Synthesis of first-strand cDNAs

Total RNA was isolated from about 100 whole adults of *D. melanogaster* strain W^{1118} using the Invitrogen TRIzol Reagent kit (Invitrogen, Rockville, MD). Further isolation of mRNA was performed using the Promega polyA + RNA isolation kit (Promega, Madison, WI). First-strand cDNA was synthesized from mRNA using a *DmNa*$_V$-specific primer (D-3′–1: 5′-tac tca tgc taa tac tcg cg-3′) based on the sequence immediately downstream of the stop codon (Genbank accession number: M32078), and Super-Script II RNase H-reverse transcriptase (Invitrogen, Rockville, MD). Conditions for the first-strand cDNA synthesis reaction were: 42°C for 2 min followed by a 60 min incubation at 48°C. RNA was removed by 20 min incubation with RNaseH at 37°C.

2.2. Polymerase chain reaction (PCR), cloning of full-length DmNa$_V$ cDNA and DNA sequencing

To amplify the complete coding region (6 kb) of *DmNa*$_V$ by PCR, a forward primer (D-DmNa$_V$-KpnI: 5′-cgg **ggt acc** gcc ***acc atg g***ca gaa gat tcc gac tcg-3′) and a reverse primer (D-DmNa$_V$-XbaI: 5′-gc**t cta g**at act gct aat act cgc g-3′) were designed based on the 5′ and 3′ end sequences of the *DmNa*$_V$ open reading frame (ORF). The *Xba*I and *Kpn*I recognition sequences (bold in the primer sequences) were added to the forward and reverse primers, respectively, to facilitate cloning. A Kozak sequence (bold-italic in the primer sequence) was added to primer D-DmNa$_V$-KpnI for high-efficiency translation. The reaction mixture (50μl) contained 0.5μl cDNA, 50 pmol each primer, 200μM each dNTP, 1 U eLONGase (Invitrogen), 1.5mM $MgCl_2$, and 1 × PCR reaction buffer. PCR was carried out as follows: one cycle of 94 °C for 1 min; 33 cycles of 94 °C for 30 s, 58 °C for 30 s, 68 °C for 8 min; and one cycle of 68 °C for 15 min. The PCR products were purified using the QIAEX II Gel Extraction Kit (QIAGEN Sciences, MD) and cloned into pGH19 (a *Xenopus* expression

vector containing the 3′ and 5′ untranslated regions of the *Xenopus β*-globin gene at the 3′ end of T7 promoter and 5′ end of SP6 promoter, respectively; and was kindly provided by B. Ganetzky, University of Wisconsin). MAX Efficiency Stbl2-competent cells (Invitrogen) were used as host cells. The DNA sequence was determined at the Research Technology Support Facility on campus using primers that anneal to both strands. Overlapping sequences were assembled and all sequence data underwent standard quality control to remove ambiguity. Sequences of *DmNa$_V$* inserts in cDNA clones were compared with the Genbank sequence (Accession number: M32078) using DNAStar (DNAStar Inc.).

2.3. Site-directed mutagenesis

Site-directed mutagenesis was performed by PCR using specific primers and Pfu Turbo DNA polymerase (Stratagene, La Jolla, CA). All mutagenesis results were verified by DNA sequencing.

2.4. Expression of DmNa$_V$ sodium channels in Xenopus oocytes

The procedures for oocyte preparation and cRNA injection were identical to those described previously (Tan et al., 2002). Plasmid DNA containing the *DmNa$_V$* insert was linearized using the *Not*I restriction enzyme. The linearized DNA was used for *in vitro* synthesis of the *DmNa$_V$* cRNA using *in vitro* transcription with T7 polymerase (mMESSAGE mMACHINE kit, Ambion). For robust expression of DmNa$_V$ sodium channels, *DmNa$_V$* cRNA (0.25–10 ng) was co-injected into oocytes with the *D. melanogaster* tipE cRNA (1:1 molar ratio), which enhances the expression of insect sodium channels in oocytes (Feng et al., 1995; Warmke et al., 1997). More than one *DmNa$_V$* and *TipE* cRNA preparations were tested for each clone with similar results. Oocytes carrying peak sodium currents of 0.5–2μA were used for functional analysis using two-electrode voltage clamp.

2.5. Electrophysiological recording and analysis

The voltage dependence of activation and inactivation were measured using the two-electrode voltage clamp technique. Methods for two-electrode recording and data analysis were similar to those described previously (Tan et al., 2002).

3. Results and discussion

3.1. Molecular analysis of 64 full-length cDNA clones

Prior to this study, molecular characterization of partial *DmNa$_V$* cDNA sequences resulted in the identification of eleven alternative exons in the *DmNa$_V$* transcript (Thackeray and Ganetzky, 1994; O'Dowd et al., 1995; Warmke et al., 1997, Lee et al., 2002). In order to determine the alternative splicing pattern of each full-length *DmNa$_V$* transcript and to conduct functional expression of each splice type, it was necessary to isolate and characterize a large number of full-length cDNA clones. Using RT-PCR, we obtained 64 full-length *DmNa$_V$* cDNA clones from adult *D. melanogaster*. PCR and/or sequencing allowed us to group the 64 clones into 29 splice types according to exon usage. Fig. 1 displays the 29 splice types (numbered 1–29) and number of clones (variants) in each splice type. Variants are named according to splice type. For example, variants in splice type 1 are designated as DmNa$_V$1, and 13 variants belonging to this splice type are named DmNa$_V$1-1 – DmNa$_V$1-13.

We found that exons a, b, d, i, j and l were used in greater than 60% of the DmNa$_V$ variants (both *D. melanogaster*), whereas usage of exons c, e, f, h and k was less frequent (Fig. 1). This observation is consistent with earlier analysis of partial cDNAs from *D. melanogaster* and *D. virilis* (O'Dowd et al., 1995;Thackeray and Ganetzky, 1994,1995). No positive or negative associations of these alternative exons with each other were observed.

3.2. Distinct gating properties of $DmNa_V$ variants expressed in Xenopus oocytes

For functional analysis of $DmNa_V$ variants, we coexpressed each variant with TipE in *Xenopus* oocytes and recorded sodium current from oocytes. Roughly half of the variants, 33, produced sodium currents large enough (0.7–2.5μA 1–8 days after cRNA injection) for further analysis. Four variants produced currents that were too small (<0.5μA) for functional analysis. Twenty-seven variants did not generate any detectable sodium current even 8 days after cRNA injection.

Analysis of the 33 functional variants revealed a broad range of voltage dependence for channel activation and inactivation (Table 1). Figs. 2A and B display the extent of variation in voltage dependence among functional $DmNa_V$ clones. The voltages for half-maximal activation ($V_{1/2}$) of most variants (76%) were within 10 mV range, between −20 and −30 mV. Six variants, $DmNa_V19$, $DmNa_V15$, $DmNa_V1$-6, $DmNa_V13$-2, $DmNa_V1$-3 and $DmNa_V2$-3, required more positive membrane potentials for activation, whereas two variants, $DmNa_V5$-1 and $DmNa_V7$-1, activated at more negative membrane potentials (Table 1). In particular, $DmNa_V7$-1 activated at voltage of <−60 mV (Fig. 2A). The so-called background sodium currents have been reported in cockroach dorsal unpaired median (DUM) neurons in terminal abdominal ganglia, which is believed to play a critical role in providing the depolarizing force needed to maintain pacemaker activity of these neurons (Lapied et al., 1990). The specific sodium channels behind such currents remain elusive. The extremely low-voltage-gating properties of $DmNa_V5$-1 and $DmNa_V7$-1 make them strong candidates for conducting background currents.

Voltages for half-maximal inactivation ($V_{1/2}$) were less variable compared with those for activation, with $V_{1/2}$ values ranging from −33 to −66 mV (Table 1 and Fig. 2B). Interestingly, the $V_{1/2}$ of inactivation of $DmNa_V7$-1 was shifted significantly in the hyperpolarizing direction compared to other variants. Inactivation was complete by the end of a 20 ms depolarization for most variants including $DmNa_V1$-1. However, five variants, $DmNa_V22$, $DmNa_V14$, $DmNa_V5$-1 and $DmNa_V7$-1 and $DmNa_V5$-3, exhibited a persistent current about 10% of the peak current remained at the end of the 20 ms depolarizing pulse, as shown for $DmNa_V7$-1 (Fig. 2C). This persistent current was also evident in the steady-state inactivation curve of $DmNa_V7$-1, where the foot of the curve is lifted at depolarizing potentials (Fig. 2B).

Surprisingly, among functional $DmNa_V$ variants, there was no apparent correlation between splice types and gating properties (Table 1, Figs. 2A and B). For example, the gating properties of six splice type 1 variants ($DmNa_V1$-1–$DmNa_V1$-6) are significantly different ($P > 0.05$) based on a one-way *ANOVA* with Scheffe's analysis. This finding suggests that other post-transcriptional modifications (e.g., RNA editing) might play a primary role in determining the voltage dependence of activation and inactivation of $DmNa_V$ variants.

3.3. Nonfunctional $DmNa_V$ variants

Although not characterized further in this study, the 31 “nonfunctional” or poorly functional clones may be a potential source for future in-depth structure–function studies of the $DmNa_V$ channel. Several explanations can be proposed for the production of nonfunctional or poorly functional variants. First, some nonfunctional variants may contain premature stop codons. While the role of truncated, nonfunctional sodium channels are not understood, specific alternative splicing events have been identified in both mammals and insects that result in nonfunctional, truncated two-domain variants (Plummer et al., 1997; Tan et al., 2002; Wang et. al., 2003). Second, some variants may contain exon b, which was previously shown in several cockroach variants to suppress sodium channel expression in *Xenopus* oocytes (Song et al., 2004). However, our analysis showed that 18 of the 32 functional

variants contain exon b (Table 1), suggesting that this exon is not the sole determinant of channel expression in *Xenopus* oocytes, but that other yet-to-be-identified sequence features are also involved. Identification of these other sequence features should improve our understanding of the mechanisms of intramolecular regulation of sodium channel gating. Third, it is also possible that some of these nonfunctional variants could be artifacts of the cloning, such as introduction of stop codon during RT-PCR cloning, or deletion of a stretch of sequence in the coding region. Finally, we used TipE as an auxiliary protein in the expression of $DmNa_V$ variants in *Xenopus* oocytes following the protocol of Warmke et al. (1997). It is possible that some variants require an auxiliary protein that is different from TipE for functional expression in this system. Recently, four *TipE*-homologous genes (*TEH1-4*) were identified in *D. melanogaster* (Derst et al., 2006). Interestingly, co-expression of three of these genes (*TEH1-3*) with a $DmNa_V$ variant in *Xenopus* oocytes elevated sodium current expression (Derst et al., 2006). In future it would be interesting to determine whether functional expression of some "nonfunctional" $DmNa_V$ variants requires a TEH protein, instead of TipE.

4. Sequence analysis of six $DmNa_V$ variants

A comprehensive sequence analysis of the 64 full-length *$DmNa_V$* clones and site-directed mutagenesis of variant-specific amino acid changes are eventually required in order to identify those specific amino acid sequences that are responsible for the gating property differences reported in this paper. Furthermore, it would be important to determine whether these specific changes are caused by RNA editing, alternative splicing, or PCR errors introduced during RT-PCR cloning. Toward this goal, we have sequenced five functional variants ($DmNa_V$5-1 and $DmNa_V$7-1, $DmNa_V$1-1, $DmNa_V$1-6 and $DmNa_V$19) that represent a wide range of gating properties (Table 2). As mentioned above, $DmNa_V$5-1 and $DmNa_V$7-1 are activated at low (i.e., more hyperpolarizing) voltages, $DmNa_V$1-6 and $DmNa_V$19 at high (i.e., more depolarizing) voltages, and $DmNa_V$1-1 at an intermediate voltage (Fig. 2 and Table 1). Because we isolated the full-length clones by RT-PCR, we expected that some of nucleotide changes would result from random PCR errors. However, such random errors are highly unlikely if a nucleotide change occurs in independent clones that belong to different splice types. Based on this criterion, we could attribute a total of nine amino acid changes (in the upper part of Table 2) to A-to-I RNA editing. Whether these changes are the result of RNA editing remain to be determined because some of the sequence differences could be caused by single-nucleotide polymorphism between the strain (unspecified) in the Genbank and strain W^{1118} used in this study.

Four of the nine A-to-I editing (Table 2) were previously reported in the *$DmNa_V$* transcript (Palladino et al., 2000). However, these RNA editing events are detected in both low-voltage-activated and high-voltage-activated variants and are therefore not likely responsible for the unique gating properties of these variants. In addition to the A-to-I editing, E299Q and L1363F were found in all five sequenced variants; both were caused by C to G changes. Finally, at the amino acid position 260, two separate changes, one from I to V and the other from I to T, were found in $DmNa_V$5-1 and $DmNa_V$7-1, respectively. Further sequencing of the corresponding regions in other 59 full-length clones reveal one more clone, $DmNa_V$4-2, which belongs to a different splice type, and also contains an I260 V change. $DmNa_V$4-2 was not functional in *Xenopus* oocytes, presumably caused by another unidentified sequence(s) in this variant. The I260 V amino acid change results from an a(tc) to g(tc) nucleotide substitution. Because it is highly unlikely that two $DmNa_V$ cDNA clones from different splice types would have the PCR errors at the same nucleotide, we concluded that the I260 V change in $DmNa_V$5-1 is caused by RNA editing. Examination of the genomic sequence of the *$DmNa_V$* gene revealed the a(tc) codon at the corresponding position. Therefore, the I260 V change is the result of A-to-I editing. Next, we conducted experiments

to determine whether the I260 V change in $DmNa_V5$-1 is responsible for the low-voltage dependence of activation. We substituted V260 with I260 in $DmNa_V5$-1. Interestingly, the V260I substitution shifted the voltage dependence of activation by 6 mV in the depolarizing direction (Fig. 2D), demonstrating that this A-to-I editing event is responsible for the low-voltage dependence of activation of $DmNa_V5$-1.

In summary, we report here the functional characterization of the largest collection of insect sodium channel variants to date. Further site-directed mutagenesis experiments are currently underway to identify potentially all amino acid changes/RNA editing events that are responsible for variant-specific gating properties. This work lays a foundation for further studies to understand the role of diverse $DmNa_V$ variants in regulating neuronal excitability in insects.

Acknowledgments

We thank Dr. Kris Silver and anonymous reviewers for critical review of this manuscript. The work was supported by a National Science Foundation Grant (IBN 9808156).

References

Byerly L, Leung HT. Ionic current of *Drosophila* neurons in embryonic cultures. J Neurosci 1988;8:4379–4393. [PubMed: 2460598]

Catterall W. From ionic currents to molecular mechanisms: the structure and function of voltage-gated sodium channels. Neuron 2000;26:13–25. [PubMed: 10798388]

Defaix A, Lapied B. Role of a novel maintained low-voltage-activated inward current permeable to sodium and calcium in pacemaking of insect neurosecretory neurons. Invert Neurosci 2005;5:135–146. [PubMed: 16177888]

Derst C, Walther C, Veh RW, Wicher D, Heinemann SH. Four novel sequences in *Drosophila melanogaster* homologous to the auxiliary $DmNa_V$ sodium channel subunit TipE. Biochem Biophys Res Commun 2006;339:939–948. [PubMed: 16325765]

Dong K. Insect sodium channels and insecticide resistance. Invert Neurosci 2007;7:17–30. [PubMed: 17206406]

Feng G, Deák P, Chopra M, Hall LM. Cloning and functional analysis of TipE, a novel membrane protein that enhances *Drosophila* $DmNa_V$ sodium channel function. Cell 1995;82:1001–1011. [PubMed: 7553842]

Goldin A, Barchi RL, Caldwell JH, Hofmann F, Howe JR, Hunter JC, Kallen RG, Mandel G, Meisler MH, Netter YB, Noda M, Tamkun MM, Waxman SG, Wood JN, Catterall WA. Nomenclature of voltage-gated sodium channels. Neuron 2000;28:365–368. [PubMed: 11144347]

Grolleau F, Lapied B. Dorsal unpaired median neurones in the insect central nervous system: towards a better understanding of the ionic mechanisms underlying spontaneous electrical activity. J Exp Biol 2000;203:1633–1648. [PubMed: 10804154]

Lapied B, Malecot CO, Pelhate M. Patch-clamp study of the properties of the sodium current in cockroach single isolated adult aminergic neurons. J Exp Biol 1990:387–403.

Lapied B, Stankiewicz M, Grolleau F, Rochat H, Zlotkin E, Pelhate M. Biophysical properties of scorpion alpha-toxin-sensitive background sodium channel contributing to the pacemaker activity in insect neurosecretory cells (DUM neurons). Eur J Neurosci 1999;11:1449–1460. [PubMed: 10103139]

Le Corronc H, Hue B, Pitman RM. Ionic mechanisms underlying depolarizing responses of an identified insect motor neuron to short periods of hypoxia. J Neurophysiol 1999;81:307–318. [PubMed: 9914291]

Lee SH, Ingles PJ, Knipple DC, Soderlund DM. Developmental regulation of alternative exon usage in the house fly Vssc1 sodium channel gene. Invert Neurosci 2002;4:125–133. [PubMed: 12488972]

Liu ZQ, Song WZ, Dong K. Persistent tetrodotoxin-sensitive sodium current resulting from U-to-C RNA editing of an insect sodium channel. Proc Natl Acad Sci USA 2004;101:11862–11867. [PubMed: 15280550]

Loughney K, Kreber R, Ganetzky B. Molecular analysis of the $DmNa_V$ locus, a sodium channel gene in *Drosophila*. Cell 1989;58:1143–1154. [PubMed: 2550145]

O'Dowd D. Voltage-gated currents and firing properties of embryonic *Drosophila* neurons grown in a chemically defined medium. J Neurobiol 1995;27:113–126. [PubMed: 7643071]

O'Dowd DK, Aldrich RW. Voltage-clamp analysis of sodium channels in wild-type and mutant *Drosophila* neurons. J Neurosci 1988;8:3633–3643. [PubMed: 2848103]

Palladino MJ, Keegan LP, O'Connell MA, Reenan RA. A-to-I pre-mRNA editing in *Drosophila* is primarily involved in adult nervous system function and integrity. Cell 2000;102:437–449. [PubMed: 10966106]

Plummer NW, McBurney MW, Meisler MH. Alternative splicing of the sodium channel SCN8A predicts a truncated two-domain protein in fetal brain and non-neuronal cells. J Biol Chem 1997;272:24008–24015. [PubMed: 9295353]

Saito M, Wu CF. Expression of ion channels and mutational effects in giant *Drosophila* neurons differentiated from cell-division arrested embryonic neuroblasts. J Neurosci 1991;11:2135–2150. [PubMed: 1712379]

Saito M, Wu CF. Ionic channels in cultures *Drosophila* neurons. EXS 1993;63:366–389. [PubMed: 7678530]

Schafer S, Rosenboom H, Menzel R. Ionic currents of Kenyon cells from the mushroom body of the honeybee. J Neurosci 1994;14:4600–4612. [PubMed: 7519255]

Song W, Liu Z, Tan J, Nomura Y, Dong K. RNA editing generates tissue-specific sodium channels with distinct gating properties. J Biol Chem 2004;279:32554–32561. [PubMed: 15136570]

Tan JG, Liu ZQ, Nomura Y, Goldin AL, Dong K. Alternative splicing of an insect sodium channel gene generates pharmacologically distinct sodium channels. J Neurosci 2002;22:5300–5309. [PubMed: 12097481]

Thackeray J, Ganetzky B. Developmentally regulated alternative splicing generates a complex array of *Drosophila* $DmNa_V$ sodium channel isoforms. J Neurosci 1994;14:2569–2578. [PubMed: 8182428]

Thackeray J, Ganetzky B. Conserved alternative splicing patterns and splicing signals in the *Drosophila* sodium channel gene $DmNa_V$. Genetics 1995;141:203–214. [PubMed: 8536968]

Wang R, Huang ZY, Dong K. Molecular characterization of an arachnid sodium channel gene from the varroa mite (*Varroa destructor*). Insect Biochem Mol Biol 2003;33:733–739. [PubMed: 12826100]

Warmke J, Reenan RA, Wang P, Qian S, Arena JP, Wang J, Wunderler D, Liu K, Kaczorowski GJ, Van der Ploeg LH, Ganetzky B, Cohen CJ. Functional expression of *Drosophila* $DmNa_V$ sodium channels. Modulation by the membrane protein TipE and toxin pharmacology. J Gen Physiol 1997;110:119–133. [PubMed: 9236205]

Wicher D, Walther C, Wicher C. Non-synaptic ion channels in insects—basic properties of currents and their modulation in neurons and skeletal muscles. Prog Neurobiol 2001;64:431–525. [PubMed: 11301158]

Yu F, Catterall WA. Overview of the voltage-gated sodium channel family. Genome Biol 2003;4:207. [PubMed: 12620097]

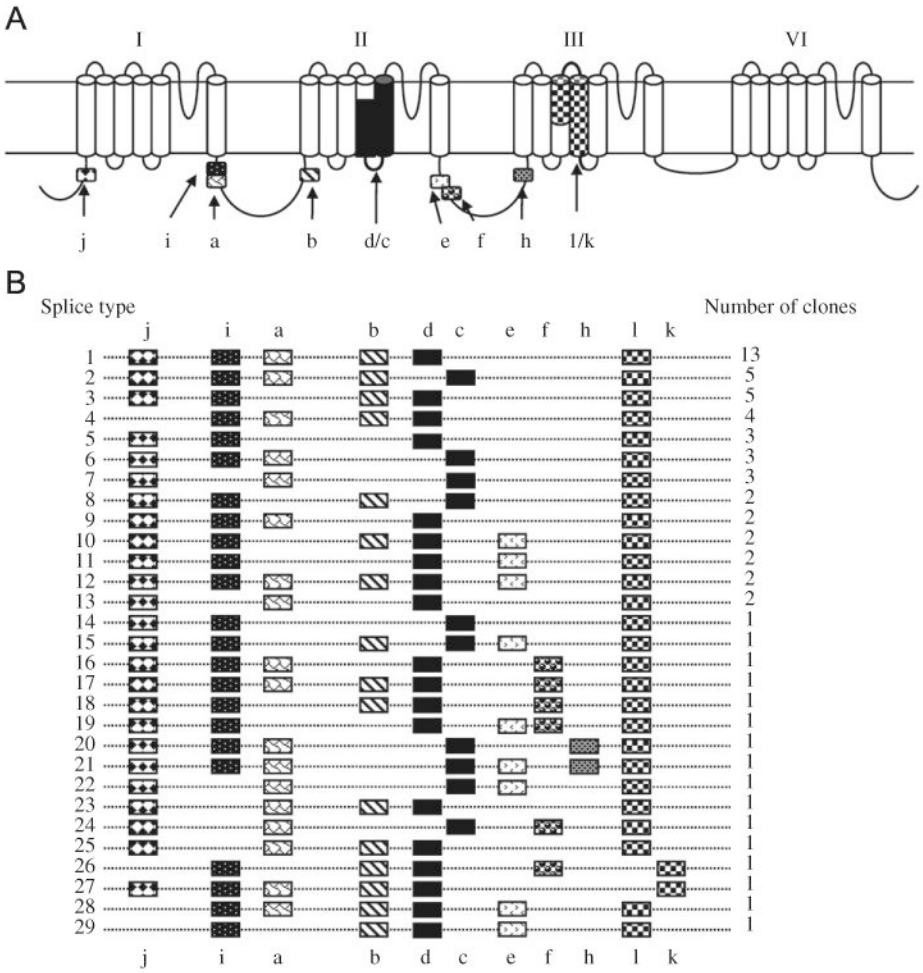

Fig. 1.

Identification of 29 alternative splice types of the $DmNa_V$ transcript. (A) A schematic diagram of the $DmNa_V$ sodium channel protein topology, with the positions of alternative exons indicated by patterned boxes. Exons, a, b, i, j, e, f and h are optional, whereas exons c/d and l/k are mutually exclusive. Exons l and k correspond to exons G1 and G2, respectively, in the cockroach BgNav sodium channel (Tan et al., 2002). (B) Schematic presentation of the usage of alternative exons in 64 full-length cDNA clones. The number of clones (i.e., variants) of each splice type is indicated.

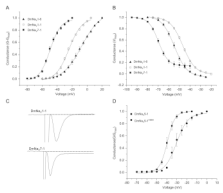

Fig. 2.

Gating properties of representative $DmNa_V$ variants. (A) Voltage dependence of activation of $DmNa_V1$-1, $DmNa_V1$-6, and $DmNa_V7$-1. (B) Voltage dependence of steady-state inactivation of $DmNa_V1$-1, $DmNa_V1$-6, and $DmNa_V7$-1. (C) Peak sodium current traces of $DmNa_V1$-1 and $DmNa_V7$-1 indicating a persistent current in $DmNa_V7$-1. (D) Voltage dependence of activation of $DmNa_V5$-1 and $DmNa_V5$-1^{V260I}.

Table 1
Gating properties of 33 functional $DmNa_V$ variants

Variant	Activation		Inactivation	
	$V_{1/2}$ (mV)	k (mV)	$V_{1/2}$ (mV)	k (mV)
$DmNa_V19$	−6.7±0.5	5.2±0.2	−50.1±0.3	6.3±0.1
$DmNa_V15$	−11.4±0.6	7.3±0.2	−34.9±0.9	5.5±0.3
$DmNa_V1$-6	−12.0±2.1	9.8±0.7	−49.9±0.5	5.6±0.9
$DmNa_V13$-2	−15.5±0.4	8.2±0.3	−45.5±0.4	7.5±0.2
$DmNa_V1$-3	−16.2±0.5	8.0±0.2	−42.3±0.6	7.3±0.6
$DmNa_V2$-3	−20.5±1.6	8.0±0.5	−46.7±0.2	4.8±0.2
$DmNa_V2$-2	−20.6±0.4	7.4±0.2	−39.8±0.4	6.1±0.2
$DmNa_V4$-1	−21.6±0.5	6.3±0.2	−41.1±0.2	5.2±0.1
$DmNa_V3$-1	−22.6±0.9	6.6±0.4	−46.4±0.4	5.0±0.1
$DmNa_V17$	−23.1±1.0	7.0±0.3	−47.4±0.6	5.1±0.2
$DmNa_V28$	−23.3±0.8	5.5±0.3	−39.9±0.5	5.4±0.2
$DmNa_V3$-2	−23.4±0.5	6.4±0.2	−43.8±0.4	5.4±0.1
$DmNa_V1$-2	−23.4±0.8	7.5±0.3	−45.1±0.4	5.5±0.1
$DmNa_V26$	−23.6±0.5	3.7±0.2	−39.7±0.2	4.4±0.1
$DmNa_V10$-2	−23.7±0.6	4.5±0.2	−40.1±0.3	4.5±0.2
$DmNa_V2$-1	−23.8±0.9	6.7±0.2	−48.3±0.5	5.3±0.1
$DmNa_V1$-1	−24.6±0.8	7.6±0.3	−47.3±0.3	5.6±0.1
$DmNa_V23$	−24.9±0.7	6.6±0.4	−46.1±0.4	5.2±0.1
$DmNa_V13$-1	−25.3±0.9	4.7±0.3	−42.9±0.3	4.8±0.1
$DmNa_V2$-4	−25.7±0.6	5.6±0.4	−46.1±0.8	4.9±0.1
$DmNa_V29$	−25.9±1.2	4.0±0.3	−38.9±0.3	4.8±0.1
$DmNa_V14$	−26.0±0.7	3.0±0.1	−32.1±0.3	4.0±0.1
$DmNa_V5$-3	−26.1±0.9	5.9±0.3	−35.1±0.6	4.9±0.1
$DmNa_V20$	−26.2±0.9	5.0±0.3	−45.1±0.3	4.9±0.1
$DmNa_V1$-5	−26.7±0.8	4.9±0.2	−43.5±0.2	4.8±0.1
$DmNa_V10$-1	−26.9±1.1	8.1±0.7	−44.8±1.1	4.8±0.8
$DmNa_V1$-4	−27.2±0.7	5.8±0.2	−45.2±0.4	5.4±0.0
$DmNa_V24$	−27.2±0.8	4.9±0.2	−41.9±0.6	5.0±0.1
$DmNa_V22$	−28.4±1.1	4.6±0.2	−42.0±0.3	5.0±0.1
$DmNa_V27$	−29.1±0.6	3.6±0.2	−42.9±0.4	4.5±0.1
$DmNa_V5$-2	−29.5±0.7	10.4±0.4	−49.2±0.5	6.5±0.3
$DmNa_V5$-1	−37.1±0.6	3.4±0.1	−44.4±0.7	4.5±0.1
$DmNa_V7$-1	−47.7±0.6	6.3±0.2	−66.4±0.2	4.5±0.0

Note: A minimum of eight oocytes was used to calculate $V_{1/2}$ and SEM values.

Table 2

Common and unique amino acid changes in five $DmNa_V$ variants

$DmNa_V1$-1	$DmNa_V7$-1	$DmNa_V5$-1	$DmNa_V19$	$DmNa_V1$-6	n.t. Δ	Location
	R52Q	R52Q	R52Q		g–**a***	N term.
E299Q	E299Q	E299Q	E299Q	E299Q	g–**c**	IS5–S6
Q471R	Q471R				**a**–g*	L1
		R1296Q	R1296Q		g–**a***	L2
		D1300N	D1300N		g–**a***	IIIS1
L1363F	L1363F	L1363F	L1363F	L1363F	g–**c**	IIIS2–S3
I1661V	I1661V	I1661V			**a**–g	IVS2
	I1670M	I1670M			**a**–g	IVS2
I1679V		I1679V		I1679V	**a**–g	IVS3
I1691V	I1691V	I1691V		I1691V	**a**–g	IVS3
N1822S		N1822S		N1822S	**a**–g	IVS5–S6
	I260T				**t**–c	IS4–S5
		I260V			**a**–g	IS4–S5
	K303R				**a**–g	IS5–S6
	W319R				**t**–c	IS5–S6
				R437K	g–**a**	L1
L486P					**t**–c	L1
		H487N			**c**–a	L1
		D656G			**a**–g	L1
M846V					a–g	IIS1–S2
				A859T	**g**–a	IIS2
				F885L	**t**–c	IIS3
			S922P		**t**–c	IIS4
V1420A					**t**–c	IIIS4–S5
				V1436A	**t**–c	IIIS5
			Q1450R		**a**–g	IIIS5
				N1463Y	**a**–t	IIIS5–S6
		I1519V			**a**–g	IIIS5–S6

$DmNa_V1$-1	**$DmNa_V7$-1**	**$DmNa_V5$-1**	**$DmNa_V19$**	**$DmNa_V1$-6**	**n.t. Δ**	**Location**
			S1587N		g–**a***	L3
	H1676R				**a**–g	IVS2–S3
	A1731V				**c**–t	IVS3
		H1772Y			**c**–t	IVS5

Note: Amino acid sequences of these variants were compared with the GenBank sequence (Genbank accession number: M32078). Nucleotide bases that correspond to these in the *$DmNa_V$* genomic sequence (FlyBase ID FBgn 003036) are in bold. Asterisks (*) represent the RNA editing events identified by Palladino et al. (2000). L1, L2, and L3 represent the three intracellular linkers connecting domains I and II, domains II and III, and domains III and IV, respectively.